SATELLITE OBSERVATIONS OF COOL OCEAN–ATMOSPHERE INTERACTION*

BY SHANG-PING XIE

New observations from space reveal surprisingly robust patterns of air–sea coupling over cool oceans where such coupling has been thought to be weak.

High sea surface temperature (SST) is generally required for deep convection that reaches the tropopause. In the current climate, the SST threshold for deep convection is somewhere around 26°–27°C, depending upon region and season (Graham and Barnett 1987; Waliser et al. 1993). Over such warm oceans, SST changes cause deep convective adjustment, which in turn excites the dynamic response of predominantly first baroclinic mode structure with strong surface wind signals. This robust relation between SST, deep convection, and wind has led to the rapid advance in understanding and modeling the tropical ocean–atmosphere interaction that gives rise to phenomena ranging from the El Niño–Southern Oscillation (ENSO; Neelin et al. 1998) to the northward displacement of the intertropical convergence zone (ITCZ; Xie and Philander 1994; Philander et al. 1996). Atmospheric general circulation models (GCMs) show considerable skills in simulating this deep adjustment to SST anomalies associated with ENSO (e.g., Alexander et al. 2002).

Over cool oceans where deep convection does not occur,[1] the atmospheric adjustment to changing SST differs markedly from that over warm oceans. Cool ocean–atmosphere interaction is poorly understood, and this lack of understanding is a stumbling block in the current effort to study non-ENSO climate variability. Unlike their success in simulating the Southern Oscillation, atmospheric GCMs disagree among themselves in their atmospheric response to SST anomalies in the extratropics (see Kushnir et al. 2002 for a review).

*International Pacific Research Center Contribution Number 239 and School of Ocean and Earth Science and Technology Contribution Number 6261.

AFFILIATION: XIE—International Pacific Research Center and Department of Meteorology, University of Hawaii at Manoa, Honolulu, Hawaii

CORRESPONDING AUTHOR: Shang-Ping Xie, IPRC/SOEST, University of Hawaii at Manoa; 1680 East West Road, Honolulu, HI 96822

E-mail: xie@hawaii.edu

DOI: 10.1175/BAMS-85-2-195

In final form 21 September 2003

©2004 American Meteorological Society

[1] While the SST threshold is a convenient way to divide the warm and cool regimes for air–sea interaction, local SST is not the only factor for deep convection, which is also influenced by other factors such as large-scale subsidence. It may be more physically appropriate to divide the warm and cold regimes according to whether there is significant deep convection or not.

Observational efforts so far have failed to yield conclusive evidence of SST effects on the planetary-scale atmospheric circulation over cool oceans because of a high level of weather noise in the extratropics on one hand, and short and sparse in situ observations on the other. Most often negative correlations between SST and surface wind speed variability are observed in the extratropics for seasonal means and on the basin scale (Fig. 1). Researchers have viewed this as being indicative of one-way forcing from atmosphere to ocean through wind-induced changes in surface turbulence heat flux (sidebar 1).

To achieve an adequate sample size in a grid box, climate datasets typically have resolutions of several hundred to 1000 km and of a month to a season. Major ocean currents like the Kuroshio and Gulf Stream are only around 100–200 km wide and form sharp SST fronts that are poorly represented in these datasets. It is on these narrow oceanic fronts, however, that ocean dynamics become important and cause large SST variations. Thus, conventional climate datasets may severely underrepresent such dynamically induced SST anomalies and their atmospheric effect.

The vast oceans can only be sparsely observed by traditional ship-based measurements, but the rapid advance in space-based microwave remote sensing is revolutionizing ocean observations, providing global fields of key ocean–atmospheric variables at unprecedented resolutions in space and time. Unlike visible and infrared remote sensing, microwave measurements are unaffected by clouds except by those with sizable precipitation. Based on microwave remote-sensing data, several recent studies have identified SST variations induced by ocean dynamics, and they have mapped the effects of these variations on the atmosphere (Xie et al. 1998; Wentz et al. 2000; Chelton et al. 2001; Xie et al. 2001; Liu 2002; White and Annis 2003; O'Neill et al. 2003; Vecchi et al. 2004). These new satellite observations reveal a rich variety of patterns of ocean–atmosphere coupling in the Indian, Pacific, and Atlantic Oceans, from the equator to the midlatitudes. Because individual papers tend to focus on one particular phenomenon in one particular region, the full spectrum of cool ocean–atmosphere interaction has not been identified.

The present paper synthesizes these recent studies and compares atmospheric response over different ocean conditions in different parts of the World Ocean. By assembling these observational facts, we wish to see whether there is a common atmospheric response pattern, and if so, by what mechanisms and under what conditions this response takes place. A synthesis of similarities and differences in the atmospheric adjustment over different regions of the World Ocean can help shed light on the dynamics of cool ocean–atmosphere interaction and stimulate future studies.

Over cool oceans, the direct effect of SST variations is likely to be trapped within the planetary boundary layer (PBL), the lowest 1–2 km of the atmosphere, because this layer is capped by a stable layer, often in

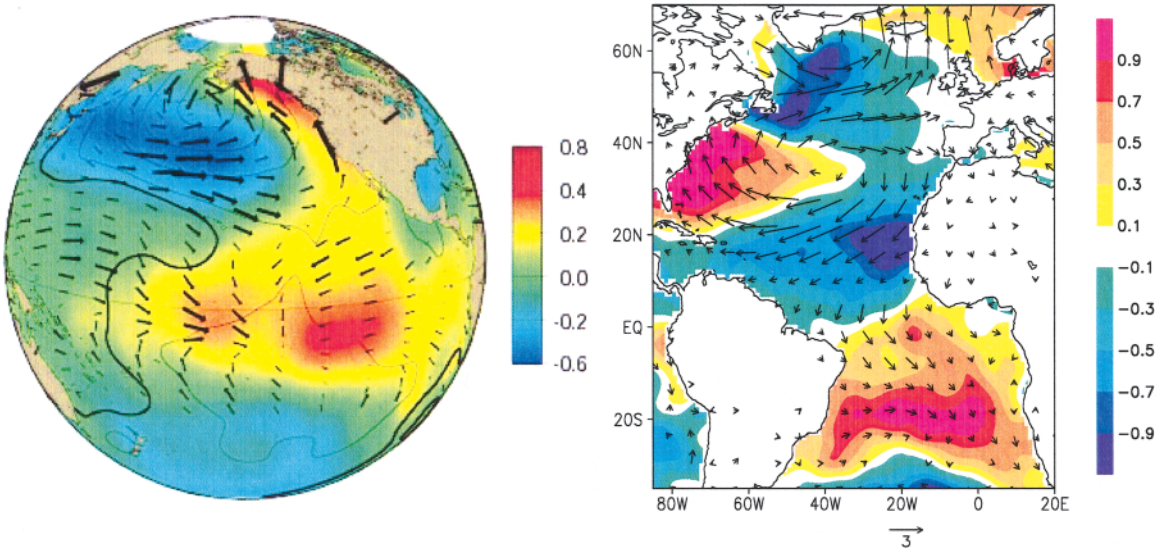

Fig. 1. SST–wind relation in the North Pacific and Atlantic Oceans. (left) COADS SST (color shade), surface wind vectors, and SLP regressed upon the Pacific decadal oscillation index (Mantua et al. 1997). (right) COADS SST (color in °C) and NCEP surface wind (m s^{-1}) composites in Jan–Mar based on a cross-equatorial SST gradient index (Okumura et al. 2001).

the form of a temperature inversion (e.g., Norris 1998). In the present review, we focus on the satellite observations of SST, surface wind velocity, and boundary layer clouds—variables most relevant to air–sea interaction. We begin with a description of the wind responses to SST variations, and then continue with a survey of cloud responses to these variations. Finally, we discuss how SST-induced anomalies in the boundary layer might lead to a deep response that reaches the upper troposphere.

Unless we mention otherwise, the following microwave measurements were used in the studies we are reviewing: sea surface vector wind by the SeaWinds scatterometer on the QuickSCAT satellite (Liu 2002); and SST, cloud water, and scalar wind speed by the Tropical Rain Measuring Mission (TRMM) satellite's microwave imager (TMI; Wentz et al. 2000). QuickSCAT data are available since July 1999 on a 0.25° grid, and TMI data since December 1997 at 0.25° resolution. QuickSCAT provides a daily coverage over 90% of the World Ocean while the TMI takes about 2 days to cover the global Tropics.

WIND RESPONSE. This section examines the SST effect on winds. We organize our discussion according to the sign and size of correlation between SST and wind speed [denoted as $r(T, W)$ hereafter], which, as will become clear, is a useful indicator of whether SST variations are merely forced by the atmosphere or whether the SST changes exert an influence on surface wind.

Positive correlation between temperature and wind speed. In the eastern equatorial Pacific and Atlantic, there is a SST front centered along 1°–2°N and separating the equatorial cold tongue from the warmer water to the north. Tropical instability waves (TIWs), due to hydrodynamic instabilities of equatorial ocean

OFF-EQUATORIAL SST VARIABILITY

With its huge heat content and slow dynamic adjustment, the ocean is generally considered as important for climate variability with time scales longer than a season. On interannual to interdecadal time scales, SST variability is generally caused by the following mechanisms: surface effects due to surface heat flux and Ekman advection that involves only the ocean mixed layer, and subsurface effects by horizontal and vertical advection due to thermocline variability. For example, the subsurface effects dominate the equatorial upwelling zone as seen in ENSO where ocean wave adjustment sets the time scale (Neelin et al. 1998).

Surface effects become dominant over open off-equatorial oceans. In particular, surface latent and sensible heat flux is generally of first-order importance over regions with a strong negative correlation between SST and wind speed as in Fig. 1. In the Tropics, because atmospheric internal variability is generally transient, two-way interaction between the ocean and atmosphere is necessary to generate modes of SST variability with preferred spatial patterns. The coupled SST–wind pattern in Fig. 1b, for example, can be maintained by a so-called wind–evaporation–SST feedback with the help of weather noise (Chang et al. 1997; Xie and Tanimoto 1998). Surface heat flux is the central agent for such a thermodynamical feedback, in contrast to the Bjerknes feedback that gives rise to ENSO with ocean dynamics as a key element. (The SST–wind relation in the equatorial Pacific near the date line in Fig. 1a is broadly consistent with the Bjerknes feedback.)

Matters become very different in the extratropics, where atmospheric internal variability is often organized in space forming stationary modes such as the Pacific–North American and North Atlantic Oscillation patterns. The temporal characteristics of such atmospheric chaotic variability are not well understood but often modeled as white noise. By simply integrating chaotic weather noise with its large heat inertia, the ocean can generate slow SST variability. Therefore, the negative correlation in Fig. 1 in the extratropics can be interpreted as ocean passively responding to wind-induced latent and sensible heat flux, with SST decreasing as the prevailing westerlies intensify (Frankignoul 1985; Barsugli and Battisti 1998).

Thus, understanding two-way ocean–atmosphere interaction in the extratropics requires answers to the following questions. First, do the ocean dynamics matter and where? Recent ocean GCM studies suggest that much of SST variability over the Kuroshio–Oyashio Extenstion (KOE) east of Japan is due to ocean dynamic effects. The deep winter mixed layer there allows the ocean memory of past wind changes to have a marked effect on SST (Xie et al. 2000) by the Rossby wave (Schneider and Miller 2001) or gyre–boundary adjustment mechanism (Seager et al. 2001). To complete the feedback loop, the second set of questions asks whether the atmosphere responds to extratropical SST variations and what feedback it provides. They are the focus of the main body of this paper.

currents, cause large meanders in this equatorial front, which propagate westward at typical wavelengths of 1000 km and typical periods of 30 days (Fig. 2a). The coupling between wind and SST is very clear in longitude–time sections (not shown; Xie et al. 1998) and discernible even on snapshot images (Fig. 2b; Chelton et al. 2001). Figure 3a shows TIW-induced SST anomalies and associated anomalous wind vectors, based on a regression analysis of Hashizume et al. (2001). Here wind speed and SST are positively correlated, with the prevailing southeasterly trade winds being accelerated over warm SST anomalies and decelerated over cold anomalies. This is opposite to the negative SST–wind correlation in Fig. 1 and represents a clear SST influence on the atmosphere. In fact, the wind speed anomalies act to dampen SST anomalies by means of surface latent- and sensible heat fluxes (Zhang and McPhaden 1995; Thum et al. 2002).

Such a positive SST–wind speed correlation is generally thought to be due to a vertical shear adjustment of the atmosphere near the sea surface (Wallace et al. 1989; Hayes et al. 1989). The increase in SST reduces the static stability of the near-surface atmosphere, causing intensified turbulent mixing that brings down fast-moving air from aloft and accelerates the surface wind. Indeed, a transect of shipboard radiosonde measurements along 2°N shows a tendency for stronger vertical shear in the lowest few hundred meters over the colder regions of the TIWs (Fig. 4).

This vertical momentum–mixing mechanism is quite ubiquitous and appears to dominate the wind adjustment to SST changes on the major ocean fronts, where we expect ocean dynamics to be the most important mechanism in causing SST variability (see sidebars 2 and 3). The characteristic positive SST–wind correlation has been detected from satellites in different regions of the World Ocean: the Atlantic equatorial front (Hashizume et al. 2001), the western north Indian Ocean (Vecchi et al. 2004), the Kuroshio and its extension (Nonaka and Xie 2003), the Southern Ocean (O'Neill et al. 2003), and the Gulf Stream rings (Park and Cornillon 2002). Marked wind speed reduction due to the same mechanism is also observed in cold wakes to typhoons that are about 100 km wide and only last for a few days (Lin et al. 2003).

Zero correlation between wind speed and temperature. Now we turn our attention to a region with a weak SST gradient. As the trade winds impinge on the Hawaiian Islands, they are blocked by the high mountains, an effect that creates a complex sequence of interactions casting a long shadow in the atmosphere and on the ocean (Fig. 3b). In this figure, the effects of the islands are isolated using a meridional filter that removes the large-scale trade wind system. The filtering reveals an anomalous band of warm SST west of Hawaii that results from the advection of warmer water from the west by an eastward current, the current itself being forced by an island-induced wind curl (Xie et al. 2001). Anomalous surface winds converge onto this warm band, indicating the in situ formation of a sea level pressure (SLP) low as a result of warming of the atmospheric boundary layer. The anomalous zonal winds are due to the bending by the Coriolis force that acts on the anomalous meridional winds or can equivalently be interpreted as geostrophic wind associated with the meridional SLP gradient.

Under the SLP-driving mechanism, the anomalous SST and winds are 90° out of phase, with the anomalous winds strengthening the prevailing northeasterly trades to the north, and weakening them to the south of the warm band. As a result, the spatial correlation between SST and wind speeds is nearly zero. In general, this lack of correlation may also result from the coexistence of one-way, basin-scale forcing of the ocean by the atmosphere [$r(T, W) < 0$] and the ocean front–induced wind covariation [$r(T, W) > 0$)], or it may simply reflect no relationship between SST and

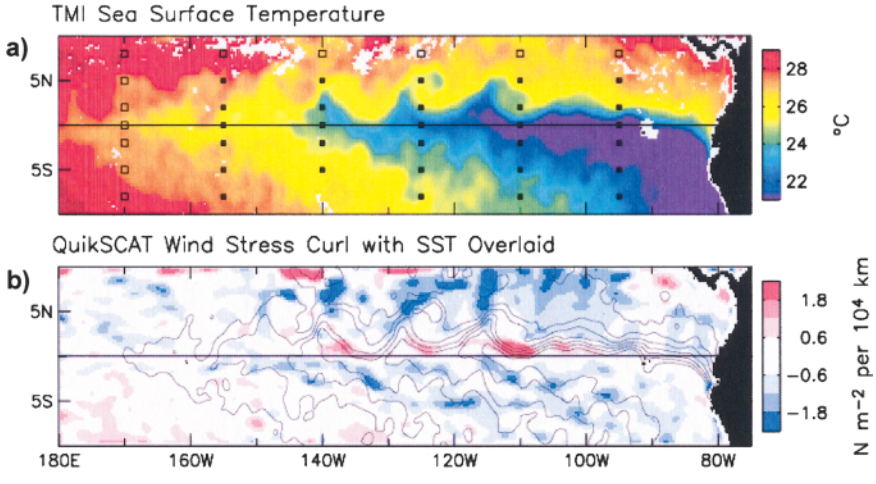

FIG. 2. TMI SST on 2–4 Sep 1999 (a) color and (b) contours. QuickSCAT wind curl with the meandering equatorial front. From Chelton et al. (2001).

wind variability. A correlation analysis between SST and wind divergence or curl will help reveal the SST-induced SLP mechanism for wind variability. (Wind convergence and curl calculations are also a spatial filter that emphasizes small-scale features such as the banded SST structure west of Hawaii.)

Thus, the SST–wind speed correlation, if statistically significant, is indeed useful in determining the causal relationship between the two. A significant positive correlation indicates that the ocean influences surface winds; a significant negative correlation in the extratropics indicates a passive SST response to changes in the atmosphere (which could be remotely forced by SST variations elsewhere, however); and a statistically insignificant correlation requires further analysis that considers lags in space or time to determine whether this lack of correlation is due to the effects of the SLP driving mechanism or is simply a reflection of random independent variations in the ocean and atmosphere.

Vertical structure of the atmosphere. Cool oceans without deep convection are often capped by a temperature inversion. The vertical displacement of the inversion results in large temperature anomalies and is important for boundary layer pressure adjustment to changing SST. In the radiosonde transect in Fig. 4, the capping inversion varies in height by as much as 500 m, from 1.5 km over the warmer regions of the TIWs to 1 km over the colder regions. A rise in the inversion height causes cold temperature anomalies in the 1- to 1.5-km layer that ride directly above the warming effect of SST anomalies. This vertical temperature dipole reduces hydrostatic pressure at the sea surface. Hashizume et al. (2002) suggest that this reduction in SLP due to the adjustment of the inversion height is the reason for the puzzling absence of pressure-driven wind anomalies over TIWs, an inference first made by Hayes et al. (1989) and subse-

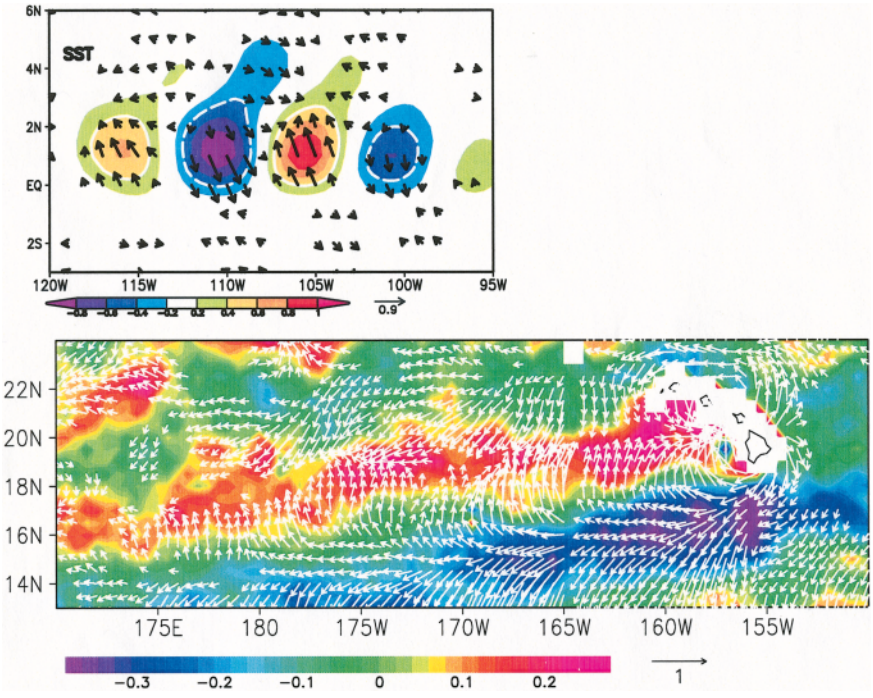

Fig. 3. Surface wind response to SST changes. (top) TMI SST (color in °C) and QuickSCAT wind (vectors in m s^{-1}) regressed upon TIW-induced SST anomalies at, 1.5°N, 105°W (Hashizume et al. 2001). (bottom) SST and wind variations induced by the presence of the Hawaiian Islands (Xie et al. 2001). Basin-scale background fields as represented by 8° meridional running means have been removed. Note the difference in SST–wind correlation from that in Fig. 1.

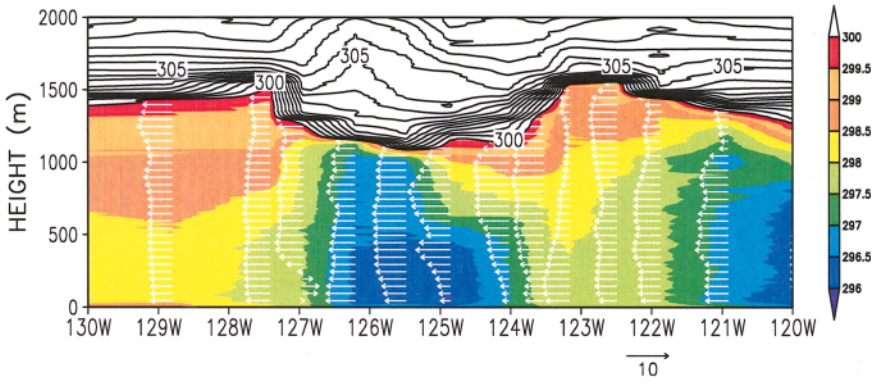

Fig. 4. Longitude–height section of virtual potential temperature (contours for $\theta_v > 300$ K and color shade for $\theta_v < 300$K) and zonal wind velocity (vectors in m s^{-1}) based on a radiosonde transect along 2°N. The survey took place during 24–25 Sep 1999.

Wind–SST coupling analogous to that on the equatorial front has recently been detected from satellite observations around the world. Some examples follow.

During June–August, the southwesterly monsoonal winds off the coast of Somalia and Arabia, called the Findlater Jet, induce strong coastal upwelling that is often associated with cold filaments extending offshore. Two such cold filaments, south and north of Socotra Island, respectively, are permanent features of summer SST climatology and act to disrupt the Findlater Jet, which has until now been depicted as a broad and continuous flow (left panel of Fig. SB1). The along-jet variations in the climatological-mean wind speed and SST are positively correlated in space and are consistent with the SST modulation of vertical mixing and wind shear (Vecchi et al. 2004).

In the extratropical North Pacific, weather noise is much greater than in the Tropics. Even there, the wind speed maximum is observed to follow the warm Kuroshio Current that takes an offshore path south of Tokyo in the right panels of Fig. SB1 (Nonaka and Xie 2003). The cold pool between Japan and the offshore Kuroshio and the cold ring farther to the east are both associated with a reduction in local wind speed.

Chelton et al. (2001) develop a quantitative procedure to test the vertical mixing mechanism for TIW-induced wind variability and show that the perturbation wind curl (divergence) is linearly proportional to the crosswind (downwind) gradient of perturbation SST. O'Neill et al. (2003) show that this proportionality holds in the circumpolar Southern Ocean (Fig. SB2), a rather surprising result considering that it is one of the stormiest oceans in the world. They average data for 3 months to suppress synoptic wind variability.

Together, these satellite studies strongly suggest that the vertical momentum mixing and the associated shear adjustment are the dominant mechanism for

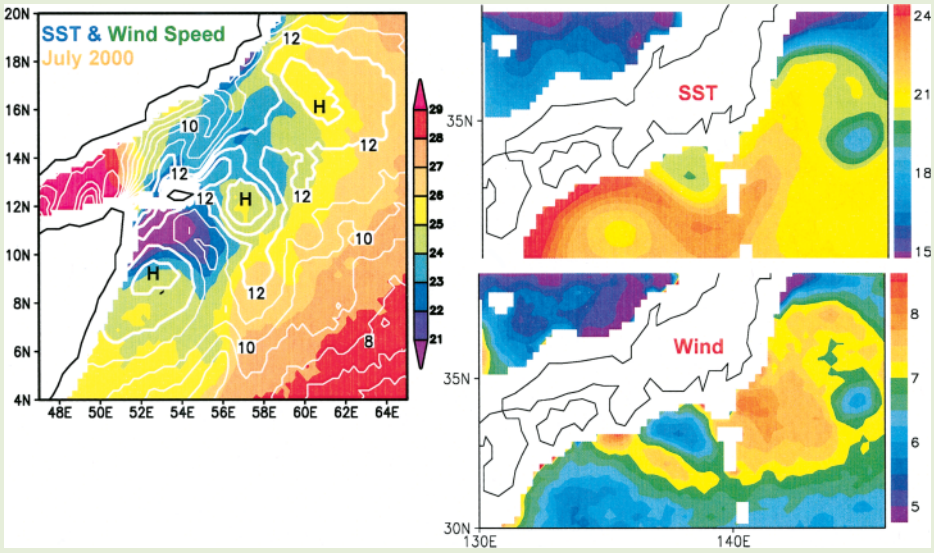

FIG. SB1. (left) TMI SST (color in °C) and wind speed (contours in m s^{-1}) averaged for Jul 2000 over the western North Indian Ocean. Note the cold wedges due to coastal upwelling and their decelerating effect on wind. (top right) TMI SST and (bottom right) wind speed over the Kuroshio Current south of Japan for Apr–Jun 2001 (Nonaka and Xie 2003). The Kuroshio appears as a stream of warm water in the SST imagery.

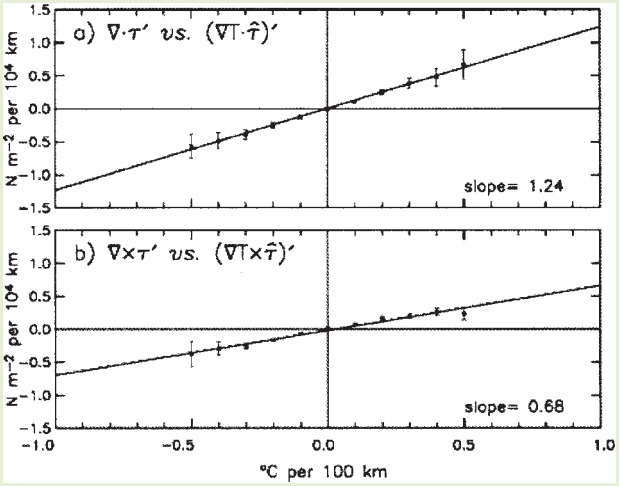

FIG. SB2. Surface wind adjustment to SST variations in the Southern Ocean. Relationship between anomalies of (a) downwind SST gradient and wind divergence and (b) crosswind SST gradient and wind curl. Spatial variations with wavelengths longer than 10° lat and 30° lon are removed. From O'Neill et al. (2003).

ocean front–PBL interaction around the world. The disparity in horizontal scale between atmospheric adjustment and oceanic fronts seems to be the main reason for the prevalence of positive SST–wind speed correlation there. Consider an idealized case of a step function oceanic front (Fig. SB3a). Dynamic adjustment of the atmosphere to this infinitesimally narrow front is likely to yield a much smoother profile of surface air temperature with finite gradients. See Warner et al. (1990) and Rogers (1989) for examples of such cross-frontal dynamic adjustment. If we assume neutral surface stability and vanishing cross-frontal wind in the background for simplicity, the resultant sea–air temperature difference is such that the warmer side of the SST front destabilizes while the colder side becomes stable. Increased mixing on the unstable warmer side reduces the near-surface wind shear, leading to an acceleration of surface winds. Such a wind acceleration has been observed in in situ measurements on the warmer flank of the Pacific equatorial front (Wallace et al. 1989) and fronts over the Gulf Stream (Sweet et al. 1981) and Kuroshio (Y. Tanimoto and H. Tokinaga 2002, personal communication).

Detailed stability distribution across the front also depends on the background cross-frontal wind. Wallace et al. (1989) propose that the thermal advection by cross-frontal mean flow is important. By this lateral advection mechanism, the vertical mixing adjustment occurs only on the downwind side of the front (Fig. SB3b). Regardless of the details of adjustment involved, large changes in stability seem common across ocean fronts.

Across ocean fronts, advection by the background winds is generally an important term in the PBL thermodynamical equations, displacing the temperature and humidity response downstream of SST anomalies. Small et al. (2003) show that such displacements lead to perturbation SLP fields with resultant wind anomalies that are positively correlated with underlying SST. This is an alternative explanation for the ubiquitous positive $r(T, W)$ correlation near fronts.

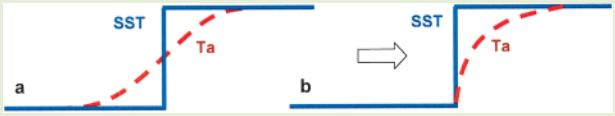

FIG. SB3. Adjustment of surface air temperature (Ta in dashed line) to a sharp SST front (solid) due to (a) gravity wave adjustment and (b) advection by the background wind (arrow). SST – Ta is positive and hence the near-surface atmosphere is more unstable on the warmer than the colder flank of the front.

quently supported by satellite measurements of surface wind[2] (Xie et al. 1998; Liu et al. 2000; Chelton et al. 2001).

Thus, the vertical structure of the atmosphere is very important for understanding the mechanisms by which it adjusts to SST variations. Because satellites do not measure vertical structure well, numerical modeling, carefully validated against observations, is a valuable tool to help us understand what is happening. For example, Fig. 5 shows the vertical structure of the atmosphere in a high-resolution regional model as it adjusts to a pair of zonal bands of positive and negative SST anomalies west of Hawaii (Hafner and Xie 2003). The air temperature in the boundary layer follows the SST anomalies imposed in the model, but at the inversion level there are considerable temperature anomalies due to the vertical displacement of the inversion. Generally, low sea level pressure forms over the warm SST band, onto which surface winds converge as in satellite observations. Two anomalous meridional circulations form with the updraft over the surface wind convergence, and they are trapped within the PBL that is capped by an inversion 2 km high. Although this circulation is shallow—only one-tenth of the tropopause height—its structure is reminiscent of the Hadley circulation and is dominated by the first baroclinic mode.

Vertically integrated, barotropic boundary layer models are often used to model surface wind velocity (e.g. Lindzen and Nigam 1987; Battisti et al. 1999), and they are successful when the boundary layer flow is connected to deeper tropospheric circulation, such as that feeding the rising branch of the Hadley cell at the ITCZ. In such cases, winds tend to flow roughly in the same direction over the depth of the boundary layer. The baroclinic response of the inversion-topped boundary layer to SST anomalies over cool oceans,

[2] Based on a high-resolution simulation, Small et al. (2003) suggest that SLP may still be an important mechanism for wind adjustment to TIW-induced SSTAs because with a small Coriolis effect near the equator, modest SLP variations can cause a large wind response. Significant SLP anomalies are indeed detected from buoy measurements, but their cause and dynamic consequences are still open to different interpretations (Cronin et al. 2003).

OCEAN DEPTH AFFECTS CLIMATE

It is well known that land shape affects weather and climate. For example, the Pacific Coast of South America is desert, while Amazonia on the other side of the Andes is rich in rainfall and hosts the largest rain forest of the world. On the global scale, the Tibetan Plateau is a controlling element in Northern Hemisphere climate. Even the tall mountains of the tiny Hawaiian Islands exert far-reaching effects on the Pacific Ocean and atmosphere.

It may sound improbable that submerged bottom topography can change winds and clouds, but satellite observations reveal a bathymetric effect over the Yellow and East China Seas (Xie et al. 2002). These seas, located between China, Korea, and Japan, together form one of the largest shelf seas of the world. Most of these seas are shallower than 100 m and their bottom topography is uneven with deeper and shallower tonguelike regions. In winter, riding on the northerly monsoon, the frigid and dry continental air blows over the seas and cools the surface. Heat is transferred from the ocean bottom upward through convection that can reach more than 100 m. The deeper the area, the more heat it contains, and the slower it cools. In this manner, the cooling rate of the water column is determined by its height. This mechanism, in combination with the advection of warm Kuroshio water by bathmetry-following shelf currents, generates warm and cold tongues over deep channels and the shallow bank, respectively.

The bathymetric effect of the seas does not stop with causing SST variations. QuickSCAT and TRMM measurements reveal remarkable spatial covariations in wind and clouds with SST. Convergent wind and increased cloudiness are found over the bathymetric-induced warm tongues. In particular, one such band of covariation between the ocean and atmosphere meanders through the Yellow Sea between China and Korea, following a deep channel for the amazing distance of 1000 km (Fig. SB4). Wind convergence is also found on the warmer flank of the Kuroshio, supporting increased CLW/precipitation there. The mechanism for this ocean effect on the winds appears to be due to the stability and wind shear adjustment similar to that over oceanic fronts (sidebar 2).

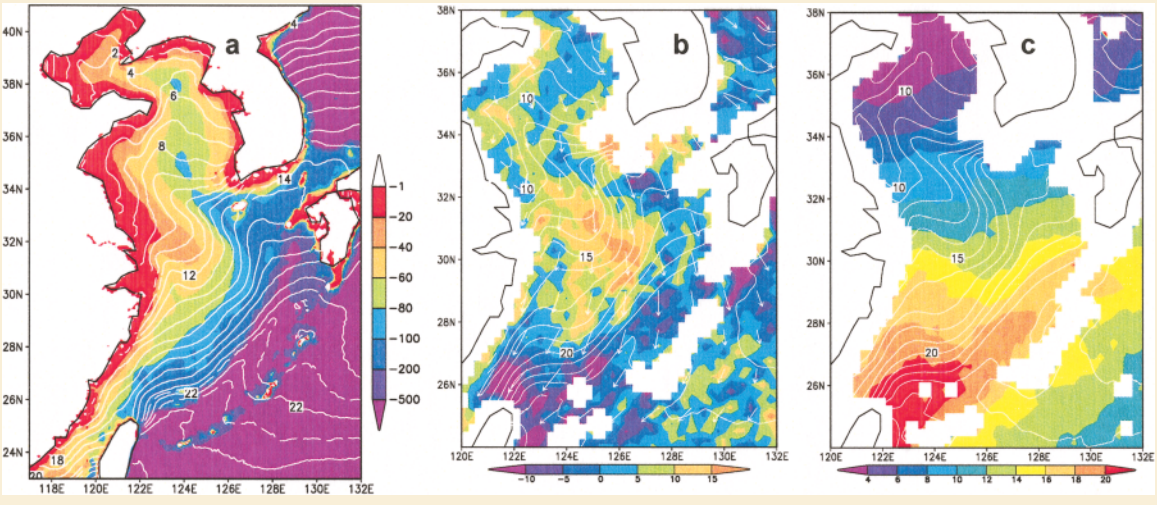

FIG. SB4. Jan–Mar SST climatology (contours in °C) over the Yellow and East China Seas, along with (a) bottom depth (m), (b) velocity (vectors in m s^{-1}) and divergence (color in 10^{-6} s^{-1}) of QuickSCAT wind, and (c) TMI cloud liquid water (10^{-2} mm). The QuickSCAT and TMI climatologies are Jan–Mar averages for 2000–02. From Xie et al. (2002).

however, calls for including baroclinic modes for surface wind simulation.

CLOUD RESPONSE. Low-level boundary layer clouds play an important role in the energy budget of the climate system. They act to cool the atmosphere by emitting longwave radiation into space as well as the ocean by reflecting solar radiation. The interaction of these low clouds with SST is complicated and poorly understood because it involves not only stability and moisture convergence but also cloud microphysics. This section presents examples of the different ways that low clouds can respond to SST anomalies.

Deser et al. (1993) first noted a correlation between clouds and TIW-induced meanders of the SST front. A detailed regression analysis of TMI data indicates

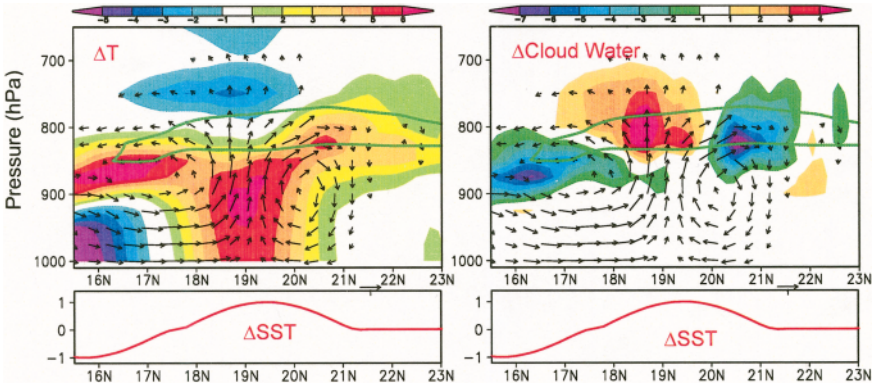

FIG. 5. Latitude–pressure section of (left) temperature (10^{-1} K), (right) cloud water content (10^{-5} kg kg^{-1}), and meridional circulation anomalies simulated in a regional atmospheric model west of HI, zonally averaged in 167°–162°W. The green contours encompass the inversion layer. SST anomalies are imposed zonally uniformly west of HI as in satellite observations (Fig. 3b) and their profile is plotted in the lower panels.

that anomalies of cloud liquid water (CLW) content are roughly but not exactly in phase with SST anomalies, with the former consistently displaced northeast of the latter (Fig. 6a). The in-phase relationship arises because intensified vertical mixing deepens the boundary layer over positive SST anomalies (Fig. 4) and transports humid surface air above the condensation level. The phase difference between CLW and SST anomalies seems to be due to surface moisture convergence; anomalous surface winds converge north of the warm SST center and diverge south of it (Fig. 3). The moisture convergence and SST effect on vertical mixing cooperate to the north of but oppose each other south of the centers of anomalous SST.

Thus, the surface wind's adjustment plays a role in how clouds respond to SST changes, and the phasing of the cloud response depends on wind response mechanisms. The vertical mixing mechanism produces wind convergence that is 90° out of phase with SST, resulting in cloud anomalies that are displaced north of SST anomalies in TIWs (Fig. 6). The SLP mechanism, on the other hand, causes wind convergence and cloud anomalies that are in phase with the SST anomalies. In the Hawaiian wake, for example, anomalous winds converge onto the warm band, leading to the formation of a cloud band collocated with the warm SST tongue west of Hawaii (Fig. 6b). Since wind velocity and CLW are measured independently, the former by QuickSCAT and the latter by TRMM satellites, the physical consistency of their covariations gives us confidence in the results. The model simulation shows that CLW increases in the anomalous updraft near the inversion height and

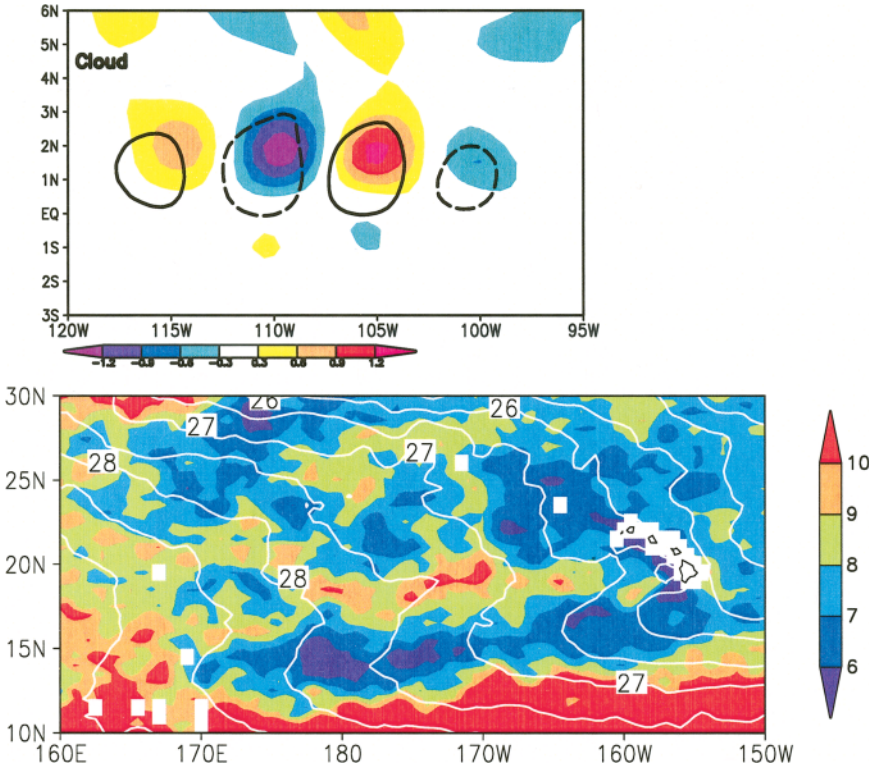

FIG. 6. Boundary layer cloud response. (top) TMI SST (contours in °C) and CLW (color in 10^{-2} mm) regressed upon TIW-induced SST anomalies at 1.5°N, 105°W (Hashizume et al. 2001). Only the 0.4°C and –0.4°C contours are plotted for SST. (bottom) TMI SST (contours in °C) and CLW (color in 10^{-2} mm) in the central subtropical North Pacific are averaged for Aug–Nov 1999 (Xie et al. 2001).

decreases in the two anomalous downdrafts (Fig. 5b).

In both TIWs and the Hawaiian wake, CLW anomalies are roughly positively correlated with and act to dampen the SST anomalies that caused the cloud changes in the first place.[3] The associated greater radiative cooling at the top of the boundary layer increases vertical turbulent mixing in the boundary layer, a cloud effect that needs further investigation. This cloud-top cooling also affects SLP and hence surface winds (Nigam 1997). (TMI measures column-integrated CLW and we have assumed that over cool oceans with a strong inversion, SST-induced CLW variability is mostly associated with low clouds.)

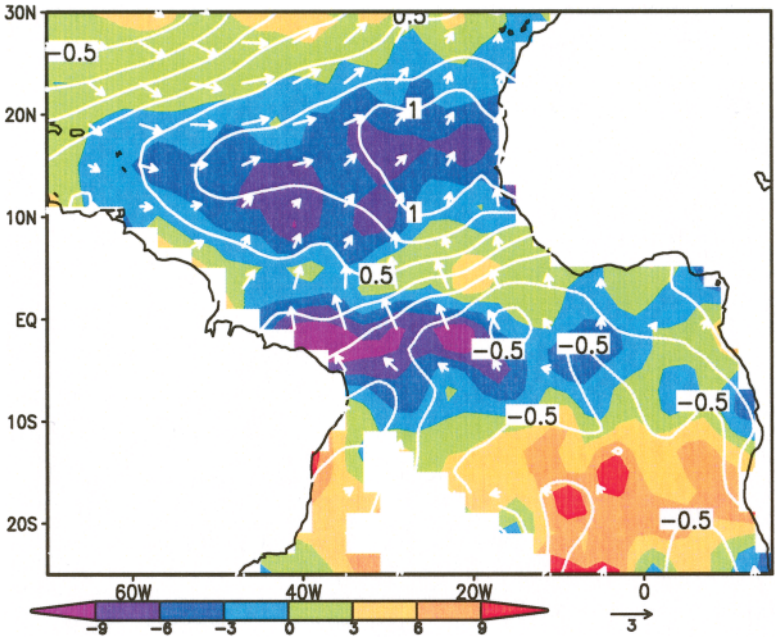

Fig. 7. COADS SST (contours in °C) and cloudiness (color in %) composites in Jan–Mar based on a cross-equatorial SST gradient index. Note that their correlation in the subtropics is opposite to that in Fig. 6.

Over many regions of the subtropical and midlatitude oceans, however, increased cloudiness is found not over warm but over cool SST anomalies (Norris and Leovy 1994; Norris et al. 1998). Figure 7 shows an example of this negative SST–cloudiness correlation in the tropical Atlantic, based on composites of ship observations with reference to a cross-equatorial SST gradient index. Associated with an anomalous basin-scale SST dipole that changes sign across the equator are four anomalous zonal cloud bands with alternating signs. The equatorial pair of cloud bands results from a warm ocean–atmosphere interaction and reflects a shift of the ITCZ rainband to the anomalously warm side of the equator. This cloud band pair is associated with strong anomalous surface wind convergence that supplies the moisture for convection. Poleward of these high-cloud changes, cloud anomalies are broadly distributed and negatively correlated with the SST anomalies underneath. Unlike the deep clouds in the ITCZ, these low-level cloud anomalies are unrelated to significant changes in surface wind convergence (Tanimoto and Xie 2002).

Klein and Hartmann (1993) found a positive correlation between low-level stratus cloud cover and the static stability of the lower troposphere. Noting that a decrease in SST increases the static stability, Philander et al. (1996) showed that this positive feedback between SST and stratus clouds helps to maintain the equatorial asymmetry of the Pacific climate. Norris (1998) suggested that this feedback is accomplished by changes in cloud types—a decrease in SST favors persistent and extensive stratocumulus clouds to more spotty trade wind cumulus clouds, thereby increasing the cloud cover. Cold advection in the boundary layer, a dominant mechanism for synoptic variability in cloudiness (Klein 1997) and large-scale subsidence above the inversion may also play a role.

Why does a rise in SST lead to an increase in low-cloud amount in one region but a decrease in another? We propose that the horizontal scale of the anomalous SST might be the key. Surface moisture convergence is inversely proportional to the spatial scale of the anomalies. Convergence is strong for small-scale SST anomalies, where it dominates other cloud-changing mechanisms, giving rise to a positive correlation with CLW. For large, basin-scale SST anomalies, moisture convergence is of secondary importance, and mechanisms such as changes in static stability take over, resulting in a negative correlation with cloudiness. This scale-dependence of moisture convergence explains why significant SST–cloudiness correlations are almost always negative around

[3] This negative feedback results from the reflection of incoming solar radiation by clouds. The presence of low clouds also increases downward infrared radiation, an effect to warm the sea surface, which Wang and Enfield (2003) suggest is important in the eastern Pacific warm pool.

the World Ocean in Norris and Leovy's (1994) coarse-resolution (10°) analysis of ship observations. Positive SST–CLW correlations, however, exist in high-resolution satellite observations over cool oceans on smaller spatial scales, as demonstrated in this review.

DISCUSSION. We have surveyed recent studies that use new satellite observations to address the questions of whether and how the atmosphere responds to SST changes over cool oceans. Our focus is on surface wind and low-level clouds, both of which are the important forcing mechanisms for SST. SST-induced vertical momentum mixing emerges as a ubiquitous mechanism by which surface wind adjusts to SST gradients at oceanic fronts in regions ranging from the equatorial cold tongue to the midlatitude North Pacific and the Southern Ocean. This vertical mixing mechanism dominates near ocean fronts because the width of these fronts is smaller than the atmospheric adjustment scale and the static stability of the near-surface atmosphere varies rapidly. It is unclear, however, how high this shear adjustment reaches. The wind speed in the lowest 100 m of the atmosphere follows a log profile that varies with static stability near the surface. Is this log-profile adjustment the main mechanism for the surface wind variations reported here or does the wind adjustment occur over the whole depth of the PBL? The radiosonde observations of TIWs in Fig. 4 suggest the latter, but more measurements and modeling studies are needed to confirm this idea.

The correlation between SST and wind speed that results from the vertical momentum mixing is positive, in contrast to the negative correlations thought to result from one-way atmospheric forcing. Thus, the SST–wind correlation turns out to be a useful indicator of the causal direction in the interaction between a cool ocean and the atmosphere. SST-induced SLP changes are another important mechanism for the generation of surface wind anomalies resulting in a zero correlation between wind speed and local SST. In such a situation, additional analysis of lagged characteristics in space and time is necessary to determine whether a causal relation between SST and wind exists.

Regarding low-level cloud response, both positive and negative correlations with SST are seen in observations. We suggest that the horizontal scale of the SST anomaly pattern is key to determining the sign of the cloud response. At small scales (a few hundred kilometers) the moisture convergence is important for cloud formation and a positive SST–cloudiness correlation tends to appear. On the basin scale, on the other hand, convergence is negligible, and the SST effect on the capping of the boundary layer becomes dominant, leading to a negative correlation between SST and cloudiness. This scale-dependence of the SST–cloudiness correlation has recently been demonstrated in a high-resolution regional atmospheric model over the southeastern tropical Pacific (H. Xu 2002, personal communication).

A natural question is how these wind and cloud responses feed back on the ocean. With increased wind speed and cloudiness over positive SST anomalies on ocean fronts, the thermal feedback is likely to be negative. The dynamic feedback is hard to assess at this time because of nonlocal wave adjustment and nonlinear processes in the ocean. The wind stress anomalies resulting from ocean front–atmosphere interactions amount to 20%–30% of the climatological mean, but because of the small spatial scale of fronts (~100 km), the wind stress curl anomalies can be as large as the mean. Figure 8 shows the 4-yr-mean

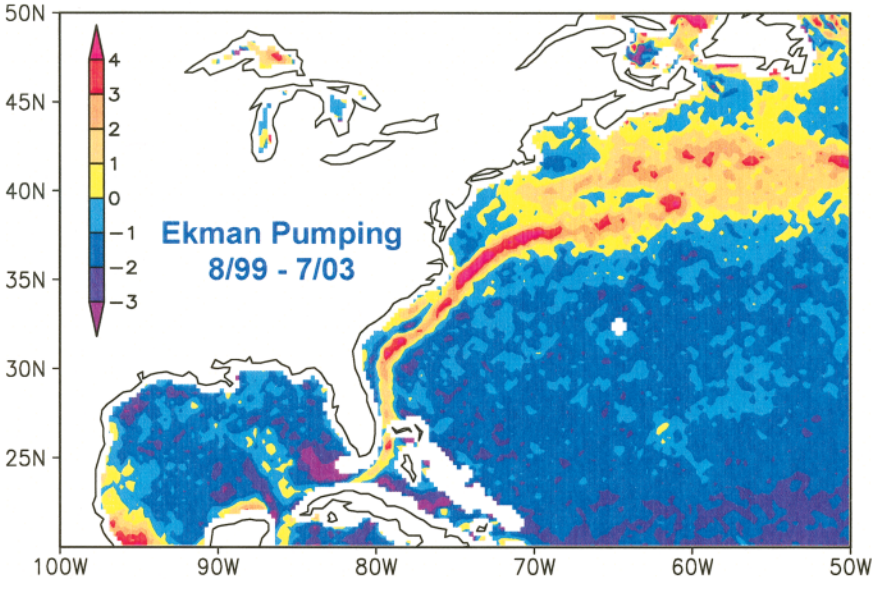

Fig. 8. Gulf Stream's effect on surface wind. Ekman pumping velocity (10^{-6} m s^{-1}) derived from QuickSCAT wind stress, averaged for 4-yr period of Aug 1999–Jul 2003.

Ekman pumping velocity derived from QuikSCAT observations, on which the effect of the warm Gulf Stream is obvious without any filter. A narrow and intense upwelling zone is found off the east coast of the United States, roughly collocated with the warm current.[4] Similar wind curls are found in the Kuroshio front in the subtropical East China Sea (sidebar 3) and along the Pacific equatorial front (Chelton et al. 2001). Such frontal-scale wind curl is neither resolved in other wind stress products nor in global GCMs, but may contribute to the recirculation of the Gulf Stream by Sverdrup dynamics (Behringer et al. 1979). Chen et al. (2003) suggest that the interaction between the SST front and the wind curls is an important element of ocean-front dynamics that strongly affects vertical nutrient transport and bioproductivity.

All the examples discussed in this paper concern the local and shallow atmospheric response that is confined to the vicinity of SST changes in the horizontal and to the boundary layer in the vertical. Important questions left unaddressed are whether this shallow boundary layer response can lead to a deep response over the whole depth of the troposphere and by what mechanism this is accomplished. Kushnir et al. (2002) review the progress and difficulty in addressing this problem of deep response. The difficulty that current globe GCMs—at typical resolutions of 2.5° in the horizontal and 500 m in the vertical—have in simulating the shallow boundary layer response may be partially responsible for their divergent results, given the strong scale dependence of this response and the importance of the inversion discussed in this paper. Most previous studies have focused on the response of stationary waves in the mid- to upper troposphere and viewed transient eddies as a feedback that amplifies and modifies the existing wave patterns. Several recent studies suggest an alternative scenario with boundary layer anomalies playing a central role. SST-induced temperature anomalies change the distribution of baroclinicity in the planetary boundary layer, which modulates the growth of transient eddies (Xie et al. 2002) and gives rise to a robust response in the storm track (Nakamura and Shimpo 2004). Transient eddies then force stationary waves by their effect on precipitation in the storm track (Inatsu et al. 2003), rather than by their sensible heat and vorticity fluxes on which many previous studies have focused.

[4] QuickSCAT measures the stress on the ocean surface. Changes in either wind or ocean currents can result in variations in QuickSCAT stress. The wind curl pattern in Fig. 8 may result from the Gulf Stream's effect on surface drag rather than its effect on surface winds (Chelton et al. 2004). Kelly et al. (2001) report a similar ocean current effect in analyzing QuickSCAT measurements over the equatorial Pacific. Taking advantage of the abundant shipboard observations over the North Atlantic east of the United States, H. Tokinaga and Y. Tanimoto (2003, personal communication) compile a new surface wind dataset and obtain an Ekman pumping field very similar to that in Fig. 8, including the narrow streak of intense upwelling along the Gulf Stream.

ACKNOWLEDGMENTS. I would like to thank D. Chelton for his helpful discussion and comments, many colleagues for their contributions to the collaborative research that this paper draws on, especially, M. Cronin, J. Hafner, H. Hashizume, M. Inatsu, W. T. Liu, H. Mukougawa, M. Nonaka, Y. Okumura, J. Small, Y. Tanimoto, and G. Vecchi. My discussion with B. Mapes was very helpful for interpreting the cloud response. Thanks are also extended to G. Speidel and anonymous reviewers for their helpful comments. This work is supported by NASA, NOAA, NSF, NSFC, and the Frontier Research System for Global Change through its support for IPRC.

REFERENCES

Alexander, M. A., I. Blade, M. Newman, J. R. Lanzante, N.-C. Lau, and J. D. Scott, 2002: The atmospheric bridge: The influence of ENSO teleconnections on air–sea interaction over the global oceans. *J. Climate,* **15,** 2205–2231.

Barsugli, J. J., and D. S. Battisti, 1998: The basic effects of atmosphere–ocean thermal coupling on midlatitude variability. *J. Atmos. Sci.,* **55,** 477–493.

Battisti, D. S., E. S. Sarachik, and A. C. Hirst, 1999: A consistent model for the large-scale steady surface atmospheric circulation in the tropics. *J. Climate,* **12,** 2956–2964.

Behringer, D., L. Regier, and H. Stommel, 1979: Thermal feedback on wind-stress as a contributing cause of the Gulf Stream. *J. Mar. Res.,* **34,** 699–709.

Chang, P., L. Ji, and H. Li, 1997: A decadal climate variation in the tropical Atlantic Ocean from thermodynamic air-sea interactions. *Nature,* **385,** 516–518.

Chelton, D. B., and Coauthors, 2001: Observations of coupling between surface wind stress and sea surface temperature in the eastern tropical Pacific. *J. Climate,* **14,** 1479–1498.

——, M. G. Schlax, M. H. Freilich, and R. F. Milliff, 2004: Satellite radar measurements reveal short-scale features in the wind stress field over the world ocean. *Science,* in press.

Chen, D., W. T. Liu, W. Tang, and Z. Wang, 2003: Air–sea interaction at an oceanic front: Implications for frontogenesis and primary production. *Geophys. Res. Lett.,* **30,** 1745, doi: 10.1029/2003GL017536.

Cronin, M. F., S.-P. Xie, and H. Hashizume, 2003: Barometric pressure variations associated with eastern Pacific tropical instability waves. *J. Climate,* **16,** 3050–3057.

Deser, C., J. J. Bates, and S. Wahl, 1993: The influence of sea surface temperature on stratiform cloudiness along the equatorial front in the Pacific Ocean. *J. Climate,* **6,** 1172–1180.

Frankignoul, C., 1985: Sea surface temperature anomalies, planetary waves, and air-sea feedback in the middle latitudes. *Rev. Geophys.,* **23,** 357–390.

Graham, N. E., and T. P. Barnett, 1987: Sea surface temperature, surface wind divergence, and convection over tropical oceans. *Science,* **238,** 657–659.

Hafner, J., and S.-P. Xie, 2003: Far-field simulation of the Hawaiian wake: Sea surface temperature and orographic effects. *J. Atmos. Sci.,* **60,** 3021–3032.

Hashizume, H., S.-P. Xie, W. T. Liu, and K. Takeuchi, 2001: Local and remote atmospheric response to tropical instability waves: A global view from the space. *J. Geophys. Res.,* **106,** 10 173–10 185.

——, ——, M. Fujiwara, M. Shiotani, T. Watanabe, Y. Tanimoto, W. T. Liu, and K. Takeuchi, 2002: Direct observations of atmospheric boundary layer response to slow SST variations on the Pacific equatorial front. *J. Climate,* **15,** 3379–3393.

Hayes, S. P., M. J. McPhaden, and J. M. Wallace, 1989: The influence of sea surface temperature on surface wind in the eastern equatorial Pacific. *J. Climate,* **2,** 1500–1506.

Inatsu, M., H. Mukougawa, and S.-P. Xie, 2003: Atmospheric response to zonal variations in midlatitude SST: Transient and stationary eddies and their feedback. *J. Climate,* **16,** 3314–3329.

Kelly, K. A., S. Dickinson, M. J. McPhaden, and G. C. Johnson, 2001: Ocean currents evident in satellite wind data. *Geophys. Res. Lett.,* **28,** 2469–2472.

Klein, S. A., 1997: Synoptic variability of low-cloud properties and meteorological parameters in the subtropical trade wind boundary layer. *J. Climate,* **10,** 2018–2039.

——, and D. L. Hartmann, 1993: The seasonal cycle of low stratiform clouds. *J. Climate,* **6,** 1587–1606.

Kushnir, Y., W. A. Robinson, I. Bladé, N. M. J. Hall, S. Peng, and R. Sutton, 2002: Atmospheric GCM response to extratropical SST anomalies: Synthesis and evaluation. *J. Climate,* **15,** 2233–2256.

Lin, I.-I., W. T. Liu, C.-C. Wu, J. C. H. Chiang, and C.-H. Sui, 2003: Satellite observations of modulation of surface winds by typhoon-induced ocean cooling. *Geophys. Res. Lett.,* **30,** 1131, doi:10.1029/2002GL015674.

Lindzen, R. S., and S. Nigam, 1987: On the role of sea surface temperature gradients in forcing low level winds and convergence in the tropics. *J. Atmos. Sci.,* **44,** 2418–2436.

Liu, W. T., 2002: Progress in scatterometer applications. *J. Oceanogr.,* **58,** 121–136.

——, X. Xie, P. S. Polito, S.-P, Xie, and H. Hashizume, 2000: Atmospheric manifestation of tropical instability waves observed by QuickSCAT and Tropical Rain Measuring Mission. *Geophys. Res. Lett.,* **27,** 2545–2548.

Mantua, N. J., S. R. Hare, Y. Zhang, J. M. Wallace, and R. C. Francis, 1997: A Pacific interdecadal climate oscillation with impacts on salmon production. *Bull. Amer. Meteor. Soc.,* **78,** 1069–1079.

Nakamura, H., and A. Shimpo, 2004: Seasonal variations in the Southern Hemisphere storm tracks and jet streams as revealed by reanalysis dataset. *J. Climate,* in press.

Neelin, J. D., D. S. Battisti, A. C. Hirst, F. F. Jin, Y. Wakata, T. Yamagata, and S. Zebiak, 1998: ENSO theory. *J. Geophys. Res.,* **103,** 14 261–14 290.

Nigam, S., 1997: The annual warm to cold phase transition in the eastern equatorial Pacific: Diagnosis of the role of stratus cloud-top cooling. *J. Climate,* **10,** 2447–2467.

Nonaka, M., and S.-P. Xie, 2003: Covariations of sea surface temperature and wind over the Kuroshio and its extension: Evidence for ocean-to-atmospheric feedback. *J. Climate,* **16,** 1404–1413.

Norris, J. R., 1998: Low cloud type over the ocean from surface observations. Part I: Relationship to surface meteorology and the vertical distribution of temperature and moisture. *J. Climate,* **11,** 369–382.

——, and C. B. Leovy, 1994: Interannual variability in stratiform cloudiness and sea surface temperature. *J. Climate,* **7,** 1915–1925.

——, Y. Zhang, and J. M. Wallace, 1998: Role of low clouds in summertime atmosphere–ocean interactions over the North Pacific. *J. Climate,* **11,** 2482–2490.

Okumura, Y., S.-P. Xie, A. Numaguti, and Y. Tanimoto, 2001: Tropical Atlantic air–sea interaction and its influence on the NAO. *Geophys. Res. Lett.,* **28,** 1507–1510.

O'Neill, L. W., D. B. Chelton, and S. K. Esbensen, 2003: Observations of SST-induced perturbations of the wind stress field over the Southern Ocean on seasonal timescales. *J. Climate,* **16,** 2340–2354.

Park, K.-A., and P. C. Cornillon, 2002: Stability-induced modification of sea surface winds over Gulf Stream

rings. *Geophys. Res. Lett.,* **29,** 2211, doi:10.1029/2001GL014236.

Philander, S. G. H., D. Gu, D. Halpern, G. Lambert, N.-C. Lau, T. Li, and R. C. Pacanowski, 1996: The role of low-level stratus clouds in keeping the ITCZ mostly north of the equator. *J. Climate,* **9,** 2958–2972.

Rogers, D. P., 1989: The marine boundary layer in the vicinity of an ocean front. *J. Atmos. Sci.,* **46,** 2044–2062.

Schneider, N., and A. J. Miller, 2001: Predicting western North Pacific Ocean climate. *J. Climate,* **14,** 3997–4002.

Seager, R., K. Kushnir, N. H. Naik, M. A. Cane, and J. Miller, 2001: Wind-driven shifts in the latitude of the Kuroshio–Oyashio extension and generation of SST anomalies on decadal timescales. *J. Climate,* **14,** 4249–4265.

Small, R. J., S.-P. Xie, and Y. Wang, 2003: Numerical simulation of atmospheric response to Pacific tropical instability waves. *J. Climate,* **16,** 3723–3741.

Sweet, W., R. Fett, J. Kerling, and P. La Violette, 1981: Air–sea interaction effects in the lower troposphere across the north wall of the Gulf Stream. *Mon. Wea. Rev.,* **109,** 1042–1052.

Tanimoto, Y., and S.-P. Xie, 2002: Inter-hemispheric decadal variations in SST, surface wind, heat flux and cloud cover over the Atlantic Ocean. *J. Meteor. Soc. Japan,* **80,** 1199–1219.

Thum, N., S. K. Esbensen, D. B. Chelton, and M. J. McPhaden, 2002: Air–sea heat exchange along the northern sea surface temperature front in the eastern tropical Pacific. *J. Climate,* **15,** 3361–3378.

Vecchi, G. A., S.-P. Xie, and A. S. Fischer, 2004: Ocean–atmosphere covariability in the western Arabian Sea. *J. Climate,* in press.

Waliser, D. E., N. E. Graham, and C. Gautier, 1993: Comparison of the highly reflective cloud and outgoing longwave radiation datasets for use in estimating tropical deep convection. *J. Climate,* **6,** 331–353.

Wallace, J. M., T. P. Mitchell, and C. Deser, 1989: The influence of sea surface temperature on surface wind in the eastern equatorial Pacific: Seasonal and interannual variability. *J. Climate,* **2,**1492–1499.

Wang, C., and D. B. Enfield, 2003: A further study of the tropical Western Hemisphere warm pool. *J. Climate,* **16,** 1476–1493.

Warner, T. T., M. N. Lakhtakia, and J. Doyle, 1990: Marine atmospheric boundary layer circulations forced by Gulf Stream sea surface temperature gradients. *Mon. Wea. Rev.,* **118,** 309–323.

Wentz, F. J., C. Gentemann, D. Smith, and D. Chelton, 2000: Satellite measurements of sea surface temperature through clouds. *Science,* **288,** 847–850.

White, W. B., and J. L. Annis, 2003: Coupling of extratropical mesoscale eddies in the ocean to westerly winds in the atmospheric boundary layer. *J. Climate,* **16,** 1095–1107.

Xie, S.-P., and S. G. H. Philander, 1994: A coupled ocean-atmosphere model of relevance to the ITCZ in the eastern Pacific. *Tellus,* **46A,** 340–350.

——, and Y. Tanimoto, 1998: A pan-Atlantic decadal climate oscillation. *Geophys. Res. Lett.,* **25,** 2185–2188.

——, M. Ishiwatari, H. Hashizume, and K. Takeuchi, 1998: Coupled ocean-atmospheric waves on the equatorial front. *Geophys. Res. Lett.,* **25,** 3863–3866.

——, T. Kunitani, A. Kubokawa, M. Nonaka, and S. Hosoda, 2000: Interdecadal thermocline variability in the North Pacific for 1958–97: A GCM simulation. *J. Phys. Oceanogr.,* **30,** 2798–2813.

——, W. T. Liu, Q. Liu and M. Nonaka, 2001: Far-reaching effects of the Hawaiian Islands on the Pacific Ocean-atmosphere. *Science,* **292,** 2057–2060.

——, J. Hafner, Y. Tanimoto, W. T. Liu, H. Tokinaga, and H. Xu, 2002: Bathymetric effect on the winter sea surface temperature and climate of the Yellow and East China Seas. *Geophys. Res. Lett.,* **29,** 2228, doi:10.1029/2002GL015884.

Zhang, G. J., and M. J. McPhaden, 1995: The relationship between sea surface temperature and latent heat flux in the equatorial Pacific. *J. Climate,* **8,** 589–605.